Numerical Investigation on the Effect of Building Overhang on the Flow within Idealised Two-dimensional Street Canyon

Muhammad Fatih bin Ibrahim[1], Mohd Faizal bin Mohamad[2], Naoki Ikegaya[3] and Azli Abd Razak[4]

[1,2,4]*School of Mechanical Engineering, College of Engineering, Universiti Teknologi MARA, Malaysia.*
[3]*Department of Energy and Environmental Engineering, Faculty of Engineering Sciences, Kyushu University, Japan.*
corresponding author: [2]*faizal3744@uitm.edu.my*

ARTICLE HISTORY	ABSTRACT
	Building overhang is an essential element in the construction of terrace houses in Malaysia to protect occupants from the sunlight, car parking, and social event purposes. However, there is still a lack of study investigating the effect of overhang in a windy area of terrace houses despite its effect on the flow modification around the building. Therefore, in this paper, a series of computational fluid dynamics (CFD) simulations were performed using Reynolds Average Navier Stokes(RANS) equations and renormalization group (RNG) k – ε as the turbulence closure model. Simulations were conducted on a unity aspect ratio of two-dimensional street canyon representing the low-rise terrace house area in a flat roof shape and three different overhang conditions. The protruding overhangs were significantly modified the in-canyon flow structure as it limited the penetration of the above flow into the canyon as compared to the without overhang case. In addition, spatially-averaged ? of the turbulent kinetic energy depicted that the value decreased within the canyon, demonstrating the independence of the overhang location. It is recommended to perform a further study on the ventilation performance of the street canyon through evaluation of ventilation indices such as ventilation rate, air exchange rate (ACH), and pollutant exchange rate (PCH).

1. INTRODUCTION

The nature of wind flow around buildings has become a major concern in recent decades because it has a significant effect on wind speed and wind direction, thereby it affects the urban area's air quality. Poor air quality can have a detrimental effect on human health. To gain a thorough understanding of the urban flow behaviour, previous researchers conducted several studies on the effect of building geometries on the airflow around the building [1–3].

The aspect ratio of the building is a critical factor in determining the wind flow within the street canyon (street width, *B* to building height, *H*) [4–5]. The street canyon's flow regime can be classified into three distinct types: isolated roughness flow (*B/H*>5.0), wake interference flow (*B/H*=1.2-5.0), and skimming flow (*B/H*=0-1.2) [5–6]. Additionally, Sini et al. [7] used a numerical simulation to determine the effect of various building aspect ratios and thermal conditions on pollutant transport behaviour. The results indicate that both factors had a significant effect on the flow structure within the street canyon by varying the number of

vortices and the vertical exchange rates. Numerical simulations of the deep canyon (*B/H*>0.1~0.66) revealthat a decrease in aspect ratio increased the number of vortices within the canyon [8–10].

Apart from that, the roof contributes to the modification of the street canyon flow pattern by determining the intensity of the in-canyon vortices [11–12]. Meanwhile, several studies [13–15] reveal that a building with a slanted pitched roof is capable to improve the ventilation performance in the street canyon. The enlargement of vortices created by the slanted roof cases aids in the penetration of wind flow from the outer layer into the canyon, so it removes the pollutant.. However, the number of vortices that are developed strongly depending on the roof shape and roof height [16–19].

Apart from the ratio and roof shape aspects, structural features such as balconies and overhangs can significantly affect the in-canyon flow. However, in urban climatology, balconies have a detrimental effect on ventilation and air quality surrounding the building [20]. Recently, Marazioti et al. [21] demonstrate that when the aspect ratio of a street canyon with balconies decreases, the ventilation also decreases. In Malaysia, overhangs are typically found among the single or two-story terrace houses and may not be available in other countries. It is constructed to provide shade, parking, and a social gathering area. The rapid growth of core housing has resulted in the development of a vast area that comprises a collection of buildings, which can be considered to resemble the urban area's topography. The main road runs through the front of the house, while the setback runs through the back, and this topography is always repeated andforming the primary feature of the urban area known as a street canyon. Although there have been several studies investigating the effect of overhang on wind flow, they have been limited to isolated buildings [22–23].

Furthermore, a series of RANS simulations over a two-dimensional street canyon demonstratethat the overhang drastically changes the canopy flow regime despite its small volume as compared to the building [24–25]. To further elucidate the mechanism of in-canyon flow structure with protruding overhang on the facades, this study employs an urban climatology approach to the terrace houses topography. Terrace houses are the assemblage of low-rise structures that can be considered to resemble an urban area with several street canyons. To conform to the existing urban climatology research, the aspect ratio is purposely designed to unite the findings for the sake of validation regarding terrace houses that are still limited. While this approach is not entirely accurate in terms of urban climatology especially for the overhang design, it is worth noting the effect of the overhang on the structure of wind flow within and above the street canyon.

2. TURBULENCE MODEL

In this study, the fully developed flow within the fluid domain was solved using three-dimensional (3D) RANS equations in conjunction with the continuity equation of this study. The RNG k-ε was selected for the turbulence closure model [26]. The continuity and steady-state RANS equations for incompressible fluid can be written as:

$$\frac{\partial \overline{u_i}}{\partial x_i} = 0 \qquad (1)$$

$$\frac{\partial(\bar{u}_i \bar{u}_j)}{\partial x_j} = -\frac{1}{\rho}\frac{\partial \bar{p}}{\partial x_i} + \frac{\partial}{\partial x_j}\left[\nu\frac{\partial \bar{u}_i}{\partial x_j} - \overline{u_i'u_j'}\right] \tag{2}$$

where the overbar denotes the mean components, $\bar{u}_i$ and $\bar{p}$, are mean velocity and pressure respectively; while ν is the fluid kinematic viscosity. Furthermore, i , $j = 1$, 2, and 3 indicate the streamwise, spanwise, and vertical directions, respectively. The Reynolds stresses are represented by $\overline{u_i'u_j'}$ and must be described in terms of mean velocity. Based on the hypothesis of the Boussinesq linear isotropic eddy-viscosity, this term can be modelled as:

$$-\overline{u_i'u_j'} = 2\nu_t S_{ij} - \frac{2}{3}k\delta_{ij} \tag{3}$$

where ν_t is the kinematic eddy viscosity; δ_{ij} is the Kronecker Delta function; and k is the turbulent kinetic energy. The stress tensor S_{ij} can be written as:

$$S_{ij} = \frac{1}{2}\left(\frac{\partial \bar{u}_i}{\partial x_j} + \frac{\partial \bar{u}_j}{\partial x_i}\right) \tag{4}$$

The transport equation for turbulent kinetic energy (TKE), *k,* and dissipation rate of turbulent kinetic energy, ε, are as below:

$$\frac{\partial}{\partial x_j}(\bar{u}_j k) = \frac{\partial}{\partial x_j}\left[\frac{\nu_t}{\sigma_k}\frac{\partial k}{\partial x_j}\right] + P_k - \varepsilon \tag{5}$$

$$\frac{\partial}{\partial x_j}(\bar{u}_j \varepsilon) = \frac{\partial}{\partial x_j}\left[\frac{\nu_t}{\sigma_\epsilon}\frac{\partial \varepsilon}{\partial x_j}\right] + \left[\left(1.42 - \frac{\eta(1-\eta/4.38)}{1+\beta\eta^3}\right)P_k - C_{\epsilon 2\epsilon}\right]\frac{\varepsilon}{k} \tag{6}$$

Here, $P_k = \nu_t S^2$ and $\eta = Sk/\varepsilon$, respectively. Other coefficients are defined as

$C_\mu = 0.0845$, $C_{\epsilon 1} = 1.42$, $C_{2\epsilon} = 1.68$, $\sigma_k = 0.71942$, $\sigma_\epsilon = 0.71942$, $\eta_0 = 4.38$, $\beta = 0.012$

3. COMPUTATIONAL DOMAIN

Figure 1 (a) shows the schematic diagram of the computational domain of this study. The domain dimension is $6H \times 4H \times 6H$ for streamwise, spanwise, and vertical direction respectively, where the building height, *H,* is 0.12m. The domain consists of three street canyons with an aspect ratio equal to 1. A similar computational domain has been employed by the previous researcher for the idealized two-dimensional flat roof building with the same boundary conditions [27]. Furthermore, all of the domain parameters follow the best practice guidelines [28–29]. The target canyon is located in the middle of the domain. The wind flow is perpendicular to the street canyon. Figure 1 (b) shows the measurement positions for the validation purpose.

Figure 2 (a) shows the canyon with no overhang used for validation and the comparison with building overhang attached either on the leeward or windward building facades (see Figure 2 (b) and (c)) of the target canyon. The thickness and length of the overhang were kept constant at $0.1H$ and $0.5H$, respectively. According to the length and position, the overhang was named as no overhang (NO), $0.5H$ leeward ($0.5HL$), and $0.5H$ windward ($0.5HW$), respectively.
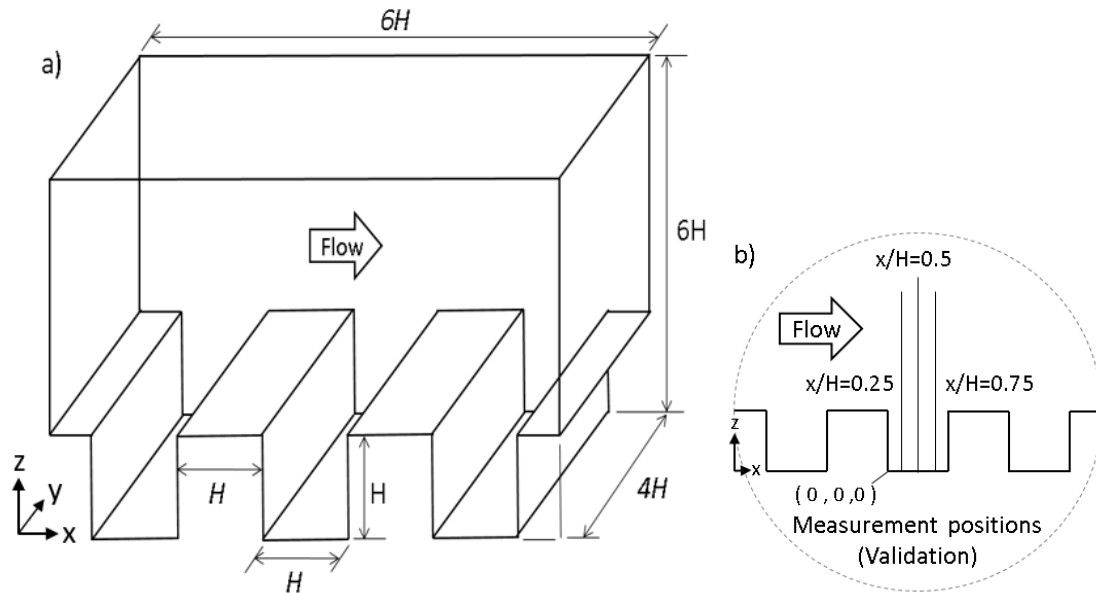
Figure 1: (a) Schematic diagram of the computational domain (b) measurement positions
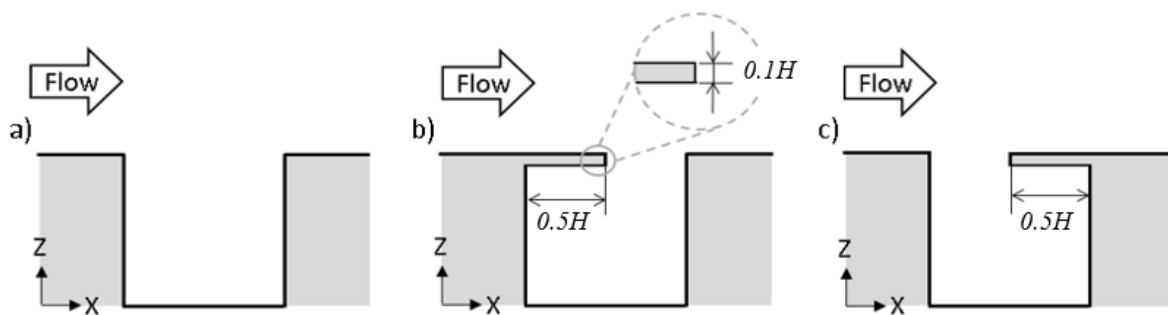

Figure 2 : Configuration of the overhang design (a) No overhang (NO) (b) 0.5*H*, leeward (0.5*HL*) (c) 0.5*H*, windward (0.5*HW*)

4. COMPUTATIONAL SETTINGS

4.1 Boundary Conditions

The periodic boundary conditions were applied on both the streamwise and spanwise boundaries, which yield infinite repeated street canyon. No-slip boundary conditions were applied at the bottom of the domain and buildings wall while the symmetry zero normal velocities and zero normal gradients were imposed on the top domain. For the ground and building surfaces, standard wall functions were applied. The flow was driven by a momentum source included in the RANS equations, u_{mean} of 8.0m/s. The Reynold number was based on the freestream flow and the building height was 576,000, which was much greater than the proposed value of 15000 [30] as it was sufficient enough for the flow to be independent of the Reynold number.

The numerical simulation was performed by using an open-source software namely OpenFOAM [31] and implementing the RANS model with RNG k-ε turbulent closure model. The flow was assumed to be steady-state, incompressible, and isothermal conditions. The

governing equations were solved by using the Semi-Implicit Method for Pressure-Linked Equations (SIMPLE) solver. Second-order accuracy was used for pressure interpolation while second-order discretization schemes were used for both convection and viscous terms of the governing equations. Convergence criteria were monitored by assigning the minimum values of the residuals to 10^{-5} for pressure and 10^{-6} for momentum, turbulent kinetic energy, and dissipation rate.

4.2 Sensitivity Analysis

To assure the results were independent of the grid size, grid sensitivity analysis was conducted for the three different meshing sizes. Domain was discretised into coarse, medium, and fine grids by varying the grid size into $H/10$, $H/20$, and $H/40$; thus, resulting in a total grid number of 132,000, 1,056,000, and 5,376,000, respectively. Figure 3 shows the velocity profiles for three different grid sizes measured at $x/H = 0.25$, 0.5, and 0.75 on the middle location of the domain.
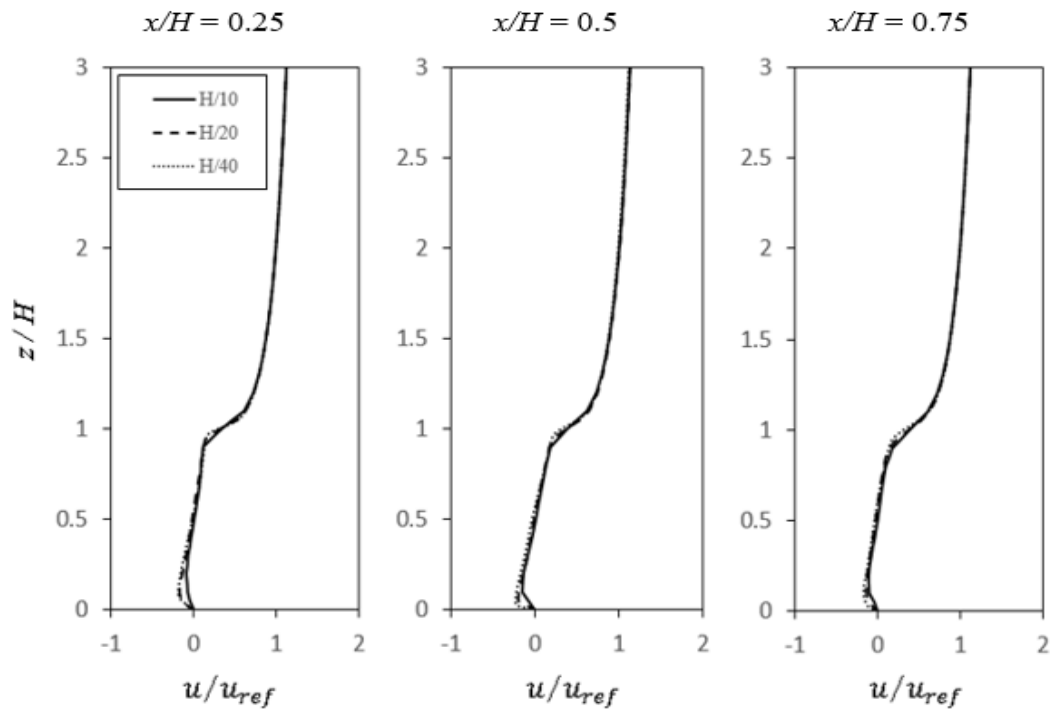

Figure 3 : Computational grid resolution comparison for grid $H/10$ (coarse), $H/20$ (medium) and $H/40$ (fine) (a) $x/H = 0.25$, (b) $x/H = 0.5$ and (c) $x/H = 0.75$. $H/10$: *solid line*, $H/20$: *dashed line* and $H/40$: *dotted line*

The horizontal axis represents the velocity, u, normalised by the reference velocity, u_{ref}, taken at two times of the building height ($z/H = 2$); while the vertical axis indicates the height, z, normalised by the building height, H. Within the canyon at $z/H < 0.25$, a significant difference can be observed as the coarse mesh (solid line) underpredicted the velocity as compared to medium (dashed line) and fine (dotted line) grids for all locations. Meanwhile, over the building height, a small discrepancy occurred at the vicinity of the building height where the shear flow was dominant. Furthermore, $z/H > 1.2$ shows almost no significant difference between all grid sizes with the increasing height. From this result, medium grid size was adopted to the rest of

the simulation by considering no significant difference with fine grid along with the computational time.

5. RESULT

5.1 Validation

The wind tunnel experiment results were carried out in a closed-circuit wind tunnel facility (TWINNEL: twinned wind tunnel) at the Central Research Institute of Electric Power Industry (CRIEPI), Japan, which were used to validate the CFD model [32]. The configuration was set up in a two-dimensional array of buildings with regularly spaced bars on the floor at a unity aspect ratio normal to the wind direction. The validation was conducted for the configuration with no overhang. Figure 4 shows the vertical profiles of the non-dimensional streamwise velocity from simulation (solid line) and experimental result (opened circle) measured in the middle of the canyon (x/H = 0.25, 0.5, and 0.75). The profiles are correctly reproduced and show a good agreement with experimental results even though there is an underprediction of the velocities magnitude within the street canyon at x/H = 0.5 and 0.75. However, the discrepancy is always lower than 6%.
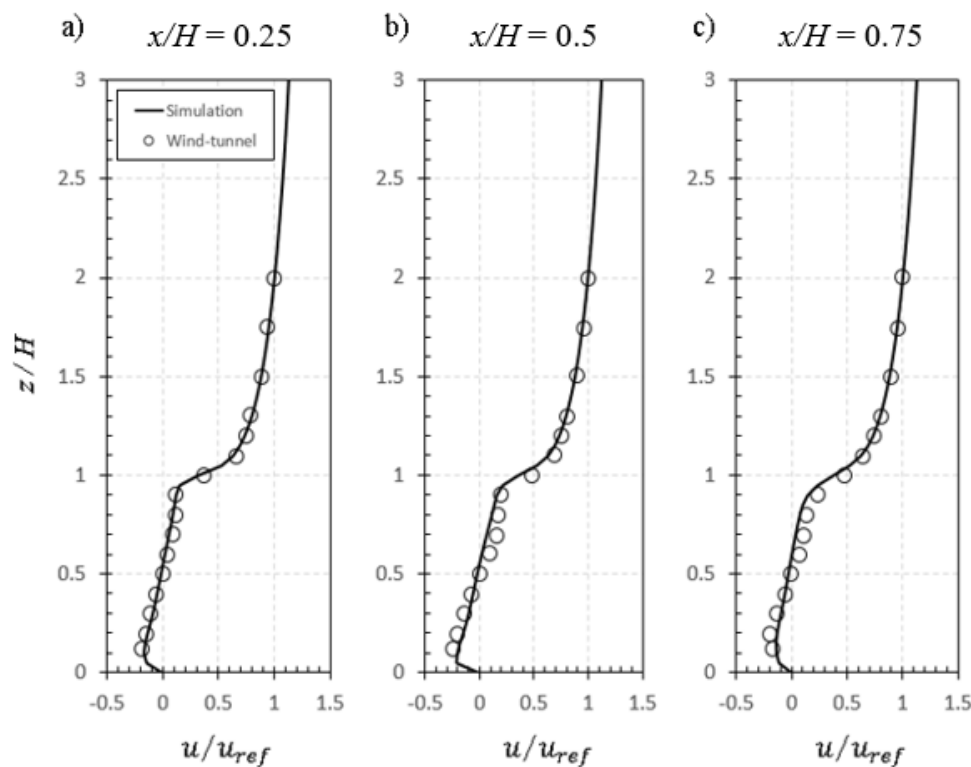

Figure 4 : Vertical distribution of the streamwise velocity at (a) x/H = 0.25, (b) x/H = 0.5 and (c) x/H = 0.75. Wind tunnel experiment: *opened circle* and current simulation: *solid line*

The distribution of the Reynolds stress estimated by using Eq. (3) is shown in Figure 5. Within the street canyon, the simulated values are comparable with the experimental results except for the lower half region at x/H = 0.75, which depicts an underprediction. At the building height, the simulation is unable to fluctuate the horizontal and vertical velocities, resulting in a low value of Reynolds stress as compared to the wind tunnel.
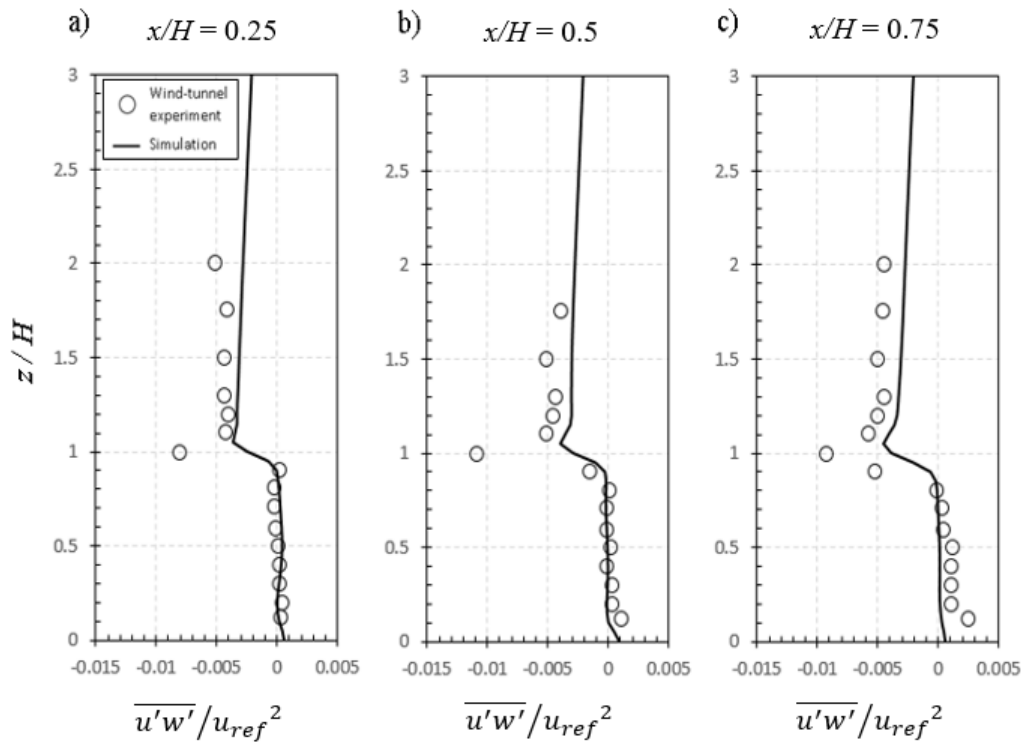
Figure 5 : Vertical distribution of Reynolds shear stress (a) *x/H* = 0.25, (b) *x/H* = 0.5 and (c) *x/H* = 0.75. Wind tunnel experiment: *opened circle* and current simulation: *solid line* (*W/H*=1)

5.2 Velocity Contour and Streamlines

Figure 6 shows the velocity streamlines in the x-z plane for all the investigated cases at the middle of the domain. For the case with no overhang (Figure 6(a)), a well-known skimming flow[33–34] with clockwise rotating vortex is generated in the centre of the canyon. The protruding overhang from the leeward façade limits the penetration of the aloft flow into the canyon, which yields modification of the in-canyon vortex (see Figure 6(b)). The vortex has diagonally deformed with the vortex centre shifted towards the windward façade. Meanwhile, in the case of overhang protrudes from the windward façade (Figure 6(c)), the primary vortex that appears in the aforementioned two cases is demolished. A small clockwise rotating vortex is developed just below the canyon opening at the top left corner.
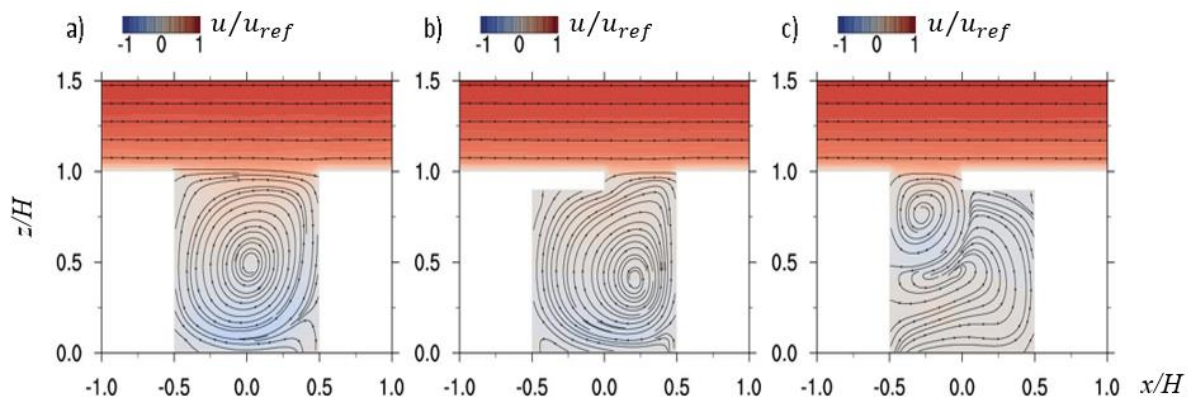

Figure 6 : Normalized velocity streamlines (a) no overhang (NO) (b) 0.5*H*, leeward (0.5*HL*) (c) 0.5*H*, windward (0.5*HW*)

5.3 Turbulent Kinetic Energy

The distribution of turbulent kinetic energy (TKE) for different overhang positions is shown in Figure 7. Intense TKE is observed at the sharp edge of the building (see Figure 7(a) and (b)) and overhang (Figure 7(c)). The TKE produced in the shear layer dissipates into the canyon along the windward façade side by the canyon vortex in the case of *NO* and 0.5*HL*. The distribution of the TKE is almost similar especially at the windward façade, but it is with a lower intensity. For the case of 0.5*HW*, TKE concentrates at the lower side of the overhang tally with the position of the vortex as anevidence of the significant velocity modification at the lower edge of the overhang. In general, TKE level is smaller for the cases with an overhang, which indicates the limited exchange of momentum between the canopy layer and the shear layer.
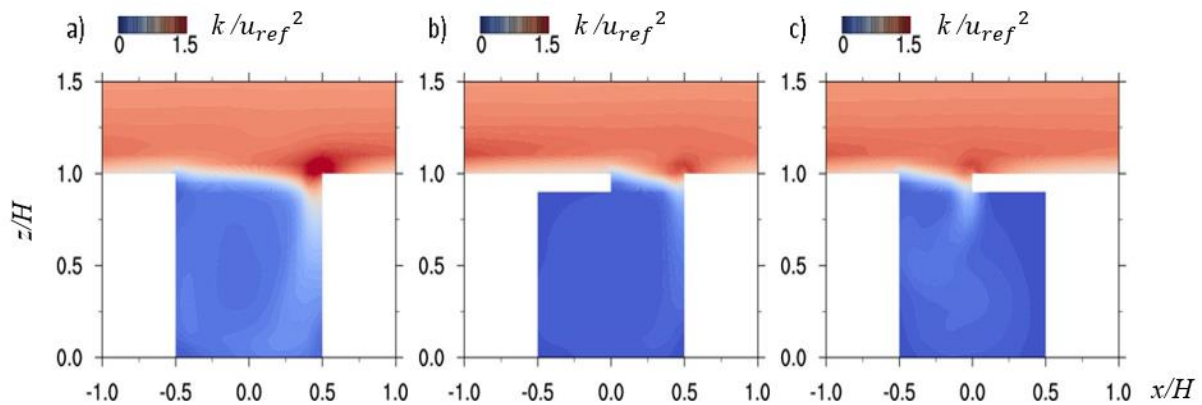

Figure 7 : Normalized turbulence kinetic energy (a) No overhang (*NO*) (b) 0.5*H*, leeward (0.5*HL*) (c) 0.5*H*, windward (0.5*HW*)

5.4 Spatially Averaged Profile

To eliminate the individual effect of the overhang that varied in the positions, spatially-averaged over target canyon was performed for the streamwise velocity and turbulence kinetic energy TKE. Figure 8(a) shows the spatially-averaged streamwise velocity normalised by the reference velocity, u_{ref}. Within the canyon ($z/H \leq 1$), a small discrepancy can be observed for all cases especially at the lower and upper regions. For a greater height $z/H > 1$, the profiles are identical. The vertical profiles of spatially-averaged turbulence kinetic energy TKE are depicted in Figure 8(b). For all cases, peaks are observed at the building height, which indicates the high strain rate due to rapid change of velocity profile resulting from the intense exchange between canopy and the shear layers. *NO* and 0.5*HW* show an identical profile that might be caused by the high strain, which occurr at the sharp edge of the downwind building and the protruded overhang, respectively. However, changing the overhang to the leeward building façade has reduced the turbulent kinetic energy. Within the canopy, *NO* case depicts the highest value as compared to the 0.5*HW* and 0.5*HL* that share nearly identical profiles. From this result, it can be concluded that even though the volume of the overhang is comparatively small concerning the building, it significantly modify the production of the turbulence kinetic energy within the canyon.
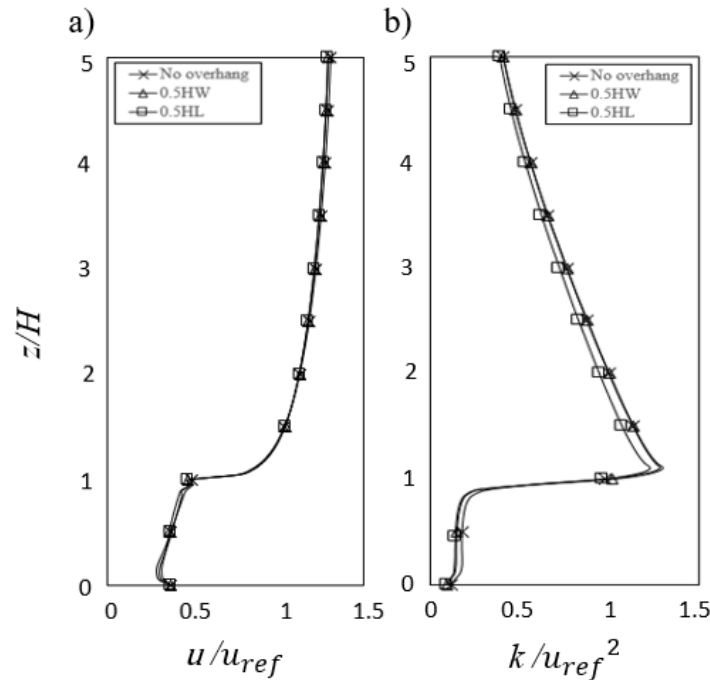
Figure 8: Vertical distribution of spatially-averaged (a) streamwise velocity (b)turbulence kinetic energy TKE. No overhang: *cross mark*, 0.5*H*, windward (0.5*HW*): *triangle* and 0.5*H*, leeward (0.5*HL*): *rectangular*

6. CONCLUSION

A series of CFD simulations were conducted to investigate the effect of building overhang that is commonly constructed on the terrace house façade through the application of urban climatology approach. In this study, three different cases were designed based on the length and position of the overhang namely no overhang (*NO*), 0.5*H*, leeward (0.5*HL*), and 0.5*H*, windward (0.5*HW*). The spatial contour of the streamwise velocity and turbulence kinetic energy show a strong dependence on the overhang position. The in-canyon vortex is significantly modified by changing the overhang position either on the windward or leeward building facades. Within the canyon, turbulence kinetic energy is reduced by the overhangs due to the limited penetration of the above flow. Spatially-averaged profiles of the streamwise velocity indicate a discrepancy within the canyon but an identical profile is observed above the canyon height. Furthermore, the turbulence kinetic energy of the NO case is the highest within the canyon; however, *NO* and 0.5*HW* share an identical profile above the building height. It is recommended to conduct further studies on the effect of varied overhang length, aspect ratio, and building geometry to elucidate the flow mechanism that will contribute to the improvement of the wind environment in the terrace house area. In addition, it is essential to evaluate the ventilation performance through the application of several indices such as ventilation rate, air exchange rate (ACH), and pollutant exchange rate (PCH).

REFERENCES

[1]   L. J. Hunter, G. T. Johnson, and I. D. Watson, "An investigation of three-dimensional characteristics of flow regimes within the urban canyon," *Atmos. Environ. Part B, Urban Atmos.*, vol. 26, no. 4, pp. 425–432, 1992, doi: 10.1016/0957-1272(92)90049-X.

[2]   X. Xie, Z. Huang, and J. S. Wang, "Impact of building configuration on air quality in street canyon," *Atmos. Environ.*, vol. 39, no. 25, pp. 4519–4530, 2005, doi: 10.1016/j.atmosenv.2005.03.043.

[3]   Y. Takano and P. Moonen, "On the influence of roof shape on flow and dispersion in an urban street canyon," *J. Wind Eng. Ind. Aerodyn.*, vol. 123, pp. 107–120, 2013, doi: 10.1016/j.jweia.2013.10.006.

[4]   F. T. DePaul and C. M. Sheih, "A study of pollutant dispersion in an urban street canyon," *Rep. ANL/ER-84-1*, pp. 84, 1984.

[5]   T. R. Oke, "Street design and urban canopy layer climate," *Energy Build.*, vol. 11, no. 1–3, pp. 103–113, 1988, doi: 10.1016/0378-7788(88)90026-6.

[6]   C. H. Chang and R. N. Meroney, "Concentration and flow distributions in urban street canyons: Wind tunnel and computational data," *J. Wind Eng. Ind. Aerodyn.*, vol. 91, no. 9, pp. 1141–1154, 2003, doi: 10.1016/S0167-6105(03)00056-4.

[7]   J. F. Sini, S. Anquetin, and P. G. Mestayer, "Pollutant dispersion and thermal effects in urban street canyons," *Atmos. Environ.*, vol. 30, no. 15, pp. 2659–2677, 1996, doi: 10.1016/1352-2310(95)00321-5.

[8]   J.-J. Baik and J.-J. Kim, "A Numerical Study of Flow and Pollutant Dispersion Characteristics in Urban Street Canyons," *J. Appl. Meteorol.*, vol. 38, no. 1988, pp. 1576–1589, 1999, doi: 10.1175/1520-0450(1999)038<1576:ANSOFA>2.0.CO;2.

[9]   S. J. Jeong and M. J. Andrews, "Application of the k-ε turbulence model to the high Reynolds number skimming flow field of an urban street canyon," *Atmos. Environ.*, vol. 36, no. 7, pp. 1137–1145, 2002, doi: 10.1016/S1352-2310(01)00569-6.

[10]   X. X. Li, C. H. Liu, and D. Y. C. Leung, "Numerical investigation of pollutant transport characteristics inside deep urban street canyons," *Atmos. Environ.*, vol. 43, no. 15, pp. 2410–2418, 2009, doi: 10.1016/j.atmosenv.2009.02.022.

[11]   S. Rafailidis, "Influence of building areal density and roof shape on the wind characteristics above a town," *Boundary-Layer Meteorol.*, vol. 85, no. 2, pp. 255–271, 1997, doi: 10.1023/A:1000426316328.

[12]   P. Kastner-Klein and E. J. Plate, "Wind-tunnel study of concentration fields in street canyons," *Atmos. Environ.*, vol. 33, no. 24–25, pp. 3973–3979, 1999, doi: 10.1016/S1352-2310(99)00139-9.

[13]   S. Ferrari, M. G. Badas, M. Garau, A. Seoni, and G. Querzoli, "The air quality in narrow two-dimensional urban canyons with pitched and flat roof buildings," *Int. J. Environ. Pollut.*, vol. 62, no. 2–4, pp. 347–368, 2017, doi: 10.1504/IJEP.2017.089419.

[14]   M. G. Badas, S. Ferrari, M. Garau, and G. Querzoli, "On the effect of gable roof on natural ventilation in two-dimensional urban canyons," *J. Wind Eng. Ind. Aerodyn.*, vol. 162, no. January, pp. 24–34, 2017, doi: 10.1016/j.jweia.2017.01.006.

[15]   M. Llaguno-Munitxa, E. Bou-Zeid, and M. Hultmark, "The influence of building geometry on street canyon air flow: Validation of large eddy simulations against wind tunnel experiments," *J. Wind Eng. Ind. Aerodyn.*, vol. 165, no. December 2016, pp. 115–130, 2017, doi: 10.1016/j.jweia.2017.03.007.

[16]   Y. Huang, M. Jin, and Y. Sun, "Numerical Studies on Airflow and Pollutant Dispersion in Urban Street Canyons Formed by Slanted Roof Buildings," *J. Hydrodyn.*, vol. 19, no. 1, pp. 100–106, 2007, doi: 10.1016/s1001-6058(07)60034-1.

[17]   Y. Huang, X. Hu, and N. Zeng, "Impact of wedge-shaped roofs on airflow and pollutant dispersion inside urban street canyons," *Build. Environ.*, vol. 44, no. 12, pp. 2335–2347, 2009, doi: 10.1016/j.buildenv.2009.03.024.

[18]   M. F. Yassin, "Impact of height and shape of building roof on air quality in urban street canyons," *Atmos. Environ.*, vol. 45, no. 29, pp. 5220–5229, 2011, doi: 10.1016/j.atmosenv.2011.05.060.

[19]   V. T. Nguyen, T. C. Nguyen, and J. Nguyen, "Numerical simulation of turbulent flow and pollutant dispersion in urban street canyons," *Atmosphere (Basel).*, vol. 10, no. 11, 2019, doi: 10.3390/atmos10110683.

[20]   D. Voordeckers, T. Lauriks, S. Denys, P. Billen, T. Tytgat, and M. Van Acker, "Guidelines for passive control of traffic-related air pollution in street canyons: An overview for urban planning," *Landsc. Urban Plan.*, vol. 207, no. June 2020, p. 103980, 2021, doi: 10.1016/j.landurbplan.2020.103980.

[21]   V. A. Karkoulias, P. E. Marazioti, D. P. Georgiou, and E. A. Maraziotis, "Computational Fluid Dynamics modeling of the trace elements dispersion and comparison with measurements in a street canyon with balconies in the city of Patras, Greece," *Atmos. Environ.*, vol. 223, no. March 2019, p. 117210, 2020, doi: 10.1016/j.atmosenv.2019.117210.

[22]   S. S. Mohaddes Foroushani, H. Ge, and D. Naylor, "Effects of roof overhangs on wind-driven rain wetting of a low-rise cubic building: A numerical study," *J. Wind Eng. Ind. Aerodyn.*, vol. 125, pp. 38–51, 2014, doi: 10.1016/j.jweia.2013.10.007.

[23]   J. I. Perén, T. van Hooff, B. C. C. Leite, and B. Blocken, "Impact of eaves on cross-ventilation of a generic isolated leeward sawtooth roof building: Windward eaves, leeward eaves and eaves inclination," *Build. Environ.*, vol. 92, pp. 578–590, 2015, doi: 10.1016/j.buildenv.2015.05.011.

[24]   M. F. Mohamad, "On The Effect Of Various Design Factors On Wind-Induced Natural Ventilation Of Residential Buildings In Malaysia," no. DECEMBER 2014, 2015.

[25]   M. F. Mohamad, A. Hagishima, N. Ikegaya, J. Tanimoto, and A. R. Omar, "Aerodynamic effect of overhang on a turbulent flow field within a two-dimensional street canyon," vol. 37, no. 1, pp. 1–7, 2015.

[26]   V. Yakhot and L. M. Smith, "The renormalization group, the ε-expansion and derivation of turbulence models," *J. Sci. Comput.*, vol. 7, no. 1, pp. 35–61, 1992, doi: 10.1007/BF01060210.

[27]   N. Saleh, M. H. M. Hashim, and M. F. Mohamad, "Large-eddy simulation of turbulent flow in an idealized street canyon," *CFD Lett.*, vol. 11, no. 11, pp. 48–57, 2019.

[28]   Y. Tominaga *et al.*, "AIJ guidelines for practical applications of CFD to pedestrian wind environment around buildings," *J. Wind Eng. Ind. Aerodyn.*, vol. 96, no. 10–11, pp. 1749–1761, 2008, doi: 10.1016/j.jweia.2008.02.058.

[29]   J. Franke, A. Hellsten, H. Schlunzen, and B. Carissimo, "Best Practice Guideline For The CFD Simulation of Flows in the Urban Environment," *COST Off.*, 2007, doi: 10.1016/S1091-255X(01)80095-0.

[30]   W. H. Snyder, "Guideline for fluid modeling of atmospheric diffusion." 1980.

[31]   H. Weller and H. Jasak, "OpenFOAM," *OpenCFD Ltd.* https://www.openfoam.com/.

[32]   T. Michioka, A. Sato, H. Takimoto, and M. Kanda, "Large-Eddy Simulation for the Mechanism of Pollutant Removal from a Two-Dimensional Street Canyon," *Boundary-Layer Meteorol.*, vol. 138, no. 2, pp. 195–213, 2011, doi: 10.1007/s10546-010-9556-2.

[33]   J.-J. Baik, R.-S. Park, H.-Y. Chun, and J.-J. Kim, "A Laboratory Model of Urban Street-Canyon Flows," *J. Appl. Meteorol.*, vol. 39, no. 9, pp. 1592–1600, 2002, doi: 10.1175/1520-0450(2000)039<1592:almous>2.0.co;2.

[34]   A. Kovar-Panskus *et al.*, "Influence of Geometry on the Mean Flow within Urban Street Canyons — A Comparison of Wind Tunnel Experiments and Numerical Simulations," *Urban Air Qual. — Recent Adv.*, no. m, pp. 365–380, 2002, doi: 10.1007/978-94-010-0312-4_26.